Materials and Structures (2017)50:158
DOI 10.1617/s11527-017-1025-7

ORIGINAL ARTICLE

Durability performance of polymeric scrap tire fibers and its reinforced cement mortar

Obinna Onuaguluchi · Nemkumar Banthia

Received: 7 July 2016 / Accepted: 14 March 2017

Abstract In this study, cement-based application for polymeric scrap tire fibers (STF) which are hitherto used either as tire derived fuel or are disposed in landfills is explored. STF was characterized; surface morphology, organic and elemental composition of STF/crumb rubber inclusions were examined. Alkaline stability of the STF, the effects of STF on plastic shrinkage cracking, mortar microstructure and long-term durability were also analyzed. Results indicate that STF which consists mainly of polyester fiber was more stable in alkaline environment compared to commercial polyethylene terephthalate (PET) fibers. Relative to the plain reference mixture, 0.4% STF and 0.3% PET fibers reduced the plastic shrinkage crack area of mortar by 97.5 and 99.4%, respectively. While inductively-coupled plasma mass spectrometer test showed that the sulfur content of the alkaline degradation test solution filtrate was <10 mg/L, scanning electron microscope–energy dispersive X-ray spectroscopy analyses revealed slight increases in the S/Ca and (Al + Fe)/Ca ratios of the specimens containing STF. However, these increased atomic ratios were insignificant; hence no degradation of the hardened properties of the STF reinforced specimens in terms of length expansion and loss of mechanical strength under accelerated curing condition and external sulfate attack were observed.

Keywords Scrap tire · Fiber · Mortar · Shrinkage · Durability · Microstructure

1 Introduction

Polymeric scrap tire fiber (STF) is one of the by-products derived from the processing of used vehicle tires. Presently, significant quantities of STF are generated annually in most developed countries of the world. However, and unfortunately, STF been an amalgam of crumb rubber, steel and other particles, its reusability has been limited. Hence, STF is mainly used as a fuel source in kilns or landfilled. A recent report by Tire Stewardship British Columbia (TSBC) [1] indicates that while a significant quantity of polymeric STF generated at a scrap tire processing plant in British Columbia was utilized as a TDF, a very small percentage of STF was landfilled.

Sulfur vulcanization of rubber is the most commonly used chemical process by which cross-links are formed between rubber polymer chains by heating, thereby enhancing the physical properties of vulcanizates. Thus, as a consequence of vulcanization, a typical tire rubber contains about 1.52–1.64% sulfur in addition to other chemical constituents such as 81.2–85.2% carbon, 7.22–7.42% hydrogen,

O. Onuaguluchi (✉) · N. Banthia
Department of Civil Engineering, University of British Columbia, 6250 Applied Science Lane, Vancouver, BC V6T 1Z4, Canada
e-mail: luchiobinna@yahoo.com

Published online: 22 March 2017

1.72–2.07% oxygen and 0.31–0.47% nitrogen [2]. According to Levendis [3], nitrogen oxides (NO_x), sulfur dioxide (SO_2), carbon monoxide (CO) and polycyclic aromatic hydrocarbon (PAH) are emitted during scrap tire combustion. Murena [4] reported that sulfur laden gases are also produced during scrap tire pyrolysis. Toxic hydrogen sulfide gas was also observed by Tang and Huang [5] as a major by-product of scrap tire pyrolysis. Therefore to avoid the inherent environmental pollution associated with the combustion of scrap tire particles attached to STF, it is imperative that alternative benign and value-added applications for STF be developed. Utilization of STF as a substitute for polymeric synthetic fibers in cement-based materials could be one of the potential applications.

Early-age cracking of cement-based materials which is traceable to capillary pore pressure induced by the evaporation of bleed surface water from a fresh mixture is a major challenge in the construction industry. Besides being aesthetically unsightly, plastic shrinkage cracks have the capacity to undermine the long-term durability performance of cement composites. Hence, in recent years, cement and concrete researchers have investigated and successfully utilized low-volume fractions of various types of synthetic fibers as a supplement to the traditional curing approach of reducing plastic shrinkage cracking in cement composites [6–8].

While the proposed reuse of STF in cement-based applications is an important step forward; however, to engender the interest and confidence of the construction industry in the quest to utilize STF in cement composites, its effects on durability properties need to be clarified. This is particularly important given that it has been reported in a recent study by Thomas and Gupta [9] that high volume fractions of crumb rubber particles in concrete reduce the long-term sulfate resistance of concrete. Previous study by Topçu and Demir [10] also reported higher degree of strength loss of rubberized mortar specimens exposed to seawater, and the authors recommended the use of high strength sulfate-resisting cement for rubberized cement composites with such exposure condition as a remedial measure. Moreover, given the conflicting reports about the resistance of polymeric fibers to alkaline degradation [11, 12], the stability of STF in alkaline cement environment is another factor that needs to be investigated.

Therefore, the objectives of this study are twofold; first, the physical morphology and chemical composition of the as-received STF were determined. Thereafter, alkaline stability of the STF, the effects of STF on the plastic shrinkage resistance of mortar and possible degradation of mortar microstructure/strength over time due to the presence of deleterious materials in STF were also investigated.

2 Experimental methods

2.1 Materials

Ordinary Portland cement (OPC) and natural sand fine aggregate having a specific gravity of 2.65 were used. STF fluffs shown in Fig. 1 were obtained from the shredding of a mixture of passenger vehicles and truck tires at Western Rubber Products Ltd. Scrap Tire Processing Plant in British Columbia, Canada. These STF fluffs were used as-received; hence they contain traces of steel and fine crumb rubber particles (approximately 51.0 wt% of STF) which were not removed during the material separation processes at the processing plant. For comparative purposes, commercial Polyethylene terephthalate (PET) monofilament fibers were also used as reinforcement in this study.

2.2 Methods

2.2.1 STF characterization

Given that vehicle tires could contain different types of synthetic fibers such as nylon, polyester, rayon and

Fig. 1 Typical scrap tire fiber fluff

etc., ASTM E1252 [13] test was performed to determine the primary organic composition of STF. The surface morphology of STF was investigated using a Scanning Electron Microscope (SEM). Furthermore, the elemental composition of the crumb rubber particles attached to STF was also evaluated using SEM—Energy Dispersive Spectroscopy (SEM–EDS) and X-ray Photoelectron Spectroscopy surface analyses. XPS analyses was performed using Omicron XPS equipment with EA125 energy analyzer, operated with the Mg Kα at 50 eV for the survey scan and 30 eV for the narrow scan.

2.2.2 *Alkaline stability of fibers*

Alkaline stability test to evaluate possible hydrolysis induced degradation of STF was undertaken. To perform this test, STF and PET fibers were immersed for 3 months in a 13.0 pH Lawrence solution ($NaOH + Ca(OH)_2 + NaCl$) which simulates typical pore solution of a cement-based material. After the 3 months immersion period, test specimens were filtered and fibers washed clean with distilled water before the surface morphology of these fibers were evaluated using SEM. Thereafter, the concentration of sulfur in filtrates as a result of the dissolution of chemical substances contained in STF-crumb rubber particles was evaluated using an inductively-coupled plasma mass spectrometer (ICP-MS). 10 ml solution samples were filtered before injection into the spectrometer. In the ICP-MS, the atoms of elements found in the filtrates are first converted to ions, before separation and detection by the mass spectrometer. From the mass spectra obtained, the concentrations of sulfur in the filtrate samples were determined. Three test replicates were performed.

2.2.3 *Mortar mixture proportion*

The first set of mixtures with water-to-cement (w/c) ratio and sand-to-cement (s/c) ratio of 0.50, and STF contents of 0, 0.2, 0.3 and 0.4% by mass of cement were used for the plastic shrinkage test. The second set of mixtures with a w/c ratio 0.50, s/c ratio of 2.0, and 0.4% STF were used for the microstructural and durability investigation. STF fluffs were first dispersed in mix water with the aid of 0.05% superplasticizer by weight of cement and a mechanical stirrer. Thereafter, cement and fine aggregate were added sequentially to the STF suspension. Plain reference and STF reinforced mortar mixtures of similar consistency were prepared using a Hobart mixer, and the total mixing time used was 6 min.

2.2.4 *Plastic shrinkage test set up and crack characterization*

The effect of STF on the restrained cracking of mortar at early-age is evaluated in this test. The Environmental Chamber used in this study measures 1705 mm × 1705 mm × 380 mm, and is equipped with temperature and humidity probes capable of regulating and monitoring the conditions inside. A constant temperature of 50 ± 1 °C and a relative humidity of about 5% were maintained inside the chamber using a three heater/blower units (240 V, 4800 W with a 1/30 HP, 1550 RPM internal electrical fan).

The restrained plastic shrinkage cracking of mortar overlay was assessed using the method proposed by Banthia and Gupta [14]. In this method, a 60 mm layer of fresh mortar was placed directly on three 40 × 95 × 325 mm fully hardened high strength concrete substrate bases. The substrate bases have 18.5 mm semicircular protuberances on the surface, which were designed to provide uniform restraint to the shrinking mortar overlays. Immediately a 60 mm deep mortar overlay was cast and troweled over the substrate bases, the substrates and the mortar overlays were transferred to the environmental chamber. After 3 h of exposure in the environmental chamber, specimens were de-molded to increase the surface area exposed to drying. Thereafter, specimens were left for an additional 21 h in the environmental chamber.

After 24 h of exposure in the environmental chamber, cracks developed on mortar overlays were characterized. For each specimen, crack widths and lengths were evaluated using image analysis software with a measurement accuracy of 0.001 mm. Based on these width and length measurements, the maximum crack width and the total crack area of the reference and the fiber reinforced specimens were determined.

2.2.5 *Microstructure, strength and phase evolution*

To investigate the possibility that contaminants attached to STF could have deleterious effects on mortar microstructure/strength on the long-term, nine

75 mm × 150 mm cylindrical specimens from each mortar mixture, moist-cured for 28 days were placed in a temperature-controlled water bath at a constant temperature of 60 °C for 3 months. Given the hot, humid and saturated environment specimens were immersed in, this curing regimen is expected to accelerate any existing degradation reaction in specimens. At monthly intervals and prior to the mechanical testing of specimens, ultrasonic pulse velocity measurements were used to evaluate the occurrence of internal cracking in specimens.

At the end of the 90 days of hot-water curing, 25 mm thick specimens cut from the mid-section of the reference and STF mechanical test cylinders were polished with four silicon carbide (SiC) polishing wheels (P120, P400, P600 and P1200) and subjected to SEM–EDS analyses using Hitachi SEM equipment. The operating conditions of the SEM equipment were 15 kV voltage and 63 µm current. Backscattered electron (BSE) images were acquired at 25 different spots in each specimen and subjected to elemental analyses. Thereafter, the atomic ratio plots of elements were used to evaluate changes in cement hydration phases in mortar samples.

2.2.6 *Sulfate resistance and longitudinal expansion of mortar*

Sulfate induced deterioration of mortar was further assessed through the time-dependent changes in mass, compressive strength and length of mortar specimens. For each mixture, three 75 mm × 150 mm cylindrical specimens moist-cured for 28 days were immersed in a 5% sodium sulfate with a pH of 6.5 and tested after 90 days immersion period. Specimens were tested in accordance with ASTM C39 [15]. Moreover, the change in length of STF reinforced specimens with steel plate mounted dial gauge attached was also monitored daily.

3 Result and discussions

3.1 STF characterization

The infrared spectra of as-received STF and known polyester fabric are shown in Fig. 2. As can be seen from Fig. 2, both spectra appear to be matched within the absorption frequency range investigated, thus

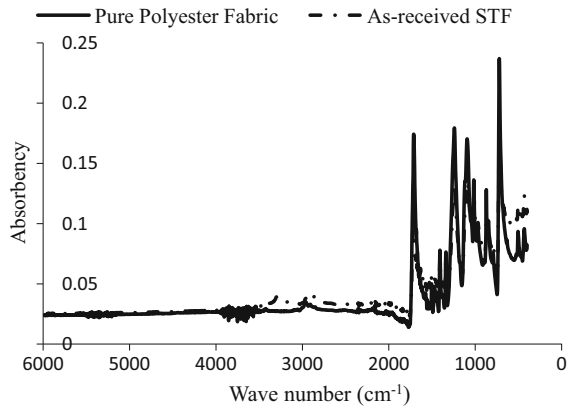

Fig. 2 Composition of scrap tire fiber fluff

suggesting that STF predominantly consists of polyester fibers. On the other hand, SEM analyses showed that while the average length of STF varied from 3 to 5 mm, the width of these fibers was in the range of 18–20 µm. Typical SEM image of a surface scarified STF is highlighted in Fig. 3. Based on the dimension of STF and its organic composition, the performance of STF reinforced mortar mixtures in this study were subsequently compared to those of mixtures containing 6 mm long, commercially available PET fibers.

Moreover, XPS narrow scan spectrum shown in Fig. 4 identified the different forms of sulfur present in crumb rubber as thiophenic and sulfate at S 2p peak binding energy corresponding to 164.1 and 168.6 eV, respectively [16, 17]. Given the well-known sulfate induced expansion of cement composites, the presence of sulfates in crumb rubber particles attached to STF is a source of concern.

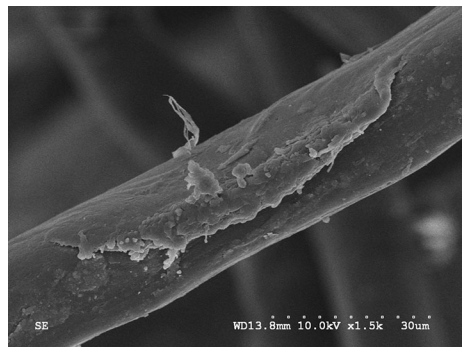

Fig. 3 Surface scarified scrap tire fiber

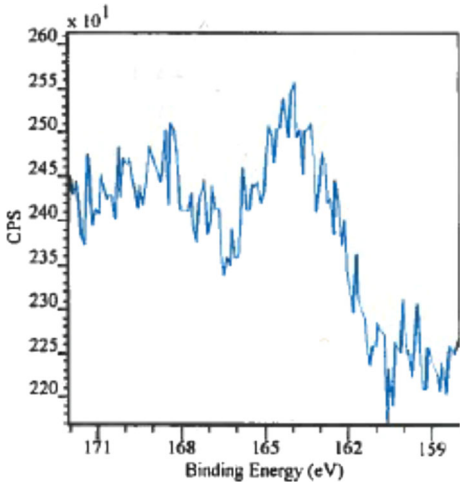

Fig. 4 XPS narrow scan spectrum of crumb rubber

3.2 Alkaline stability of fibers

The SEM micrographs shown in Fig. 5a, b show surface degradation of both STF and PET fibers after 3 months exposure to an alkaline solution of 13.0 pH. However, while the PET fibers show evidence of significant pitting corrosion and roughening on the surface, the surface of the STF appeared less roughened and damaged. However, considerable peeling off deterioration in STF that were already scarified before immersion in the alkaline solution was also observed. Although these results are consistent with previous research findings [18, 19] that polyester fiber degrades in strong alkaline environments, the superior performance of the STF relative to the PET fiber in alkaline solution is ascribed to the presence of polymeric cord/rubber interfacial adhesion promoting resorcinol–formaldehyde–latex (RFL) and other intermediary dip coatings on its surface. Jamshidi et al. [20] were of the opinion that heat-cured RFL dip are not only insoluble, it also enhances the flexibility, heat and fatigue resistance of cords.

3.3 Plastic shrinkage

Visual inspection of specimens indicates that the addition of STF and PET fibers to mortar mixtures reduced plastic shrinkage cracking significantly. Compared to the large transverse through cracks observed in the reference specimens, fiber reinforced specimens seem to have small-sized and segmented multiple cracks. Figure 6 shows that none of the specimens containing either STF or PET fibers had cracks that were wider than 0.7 mm. Moreover, while the reductions in maximum crack width in comparison to the reference mortar ranged from 86.4 to 93.2% for specimens containing 0.1–0.3% PET fibers, the reductions in maximum crack width in comparison to the reference mixture for specimens containing 0.1–0.4% STF were 52.7, 68.2, 72.4 and 92.7%, respectively.

The total crack area of specimens is shown in Fig. 7, and it indicates that both fibers were very effective in reducing plastic shrinkage cracking. Compared to the reference specimens, while the addition of 0.1–0.4% STF to mixtures induced approximately 74–97.5% reduction in total crack area, the reductions in total crack area of specimens containing 0.1–0.3% PET fibers varied from 96 to 99.4%. Therefore, it seems that the optimum fiber contents for PET and STF are 0.2 and 0.4%, respectively. The main reasons for the enhanced crack resistance of specimens reinforced with both types of fibers are the increased ductility of the mortar matrix and the crack bridging ability of the fibers which limits crack initiation and propagation. Reduction in matrix

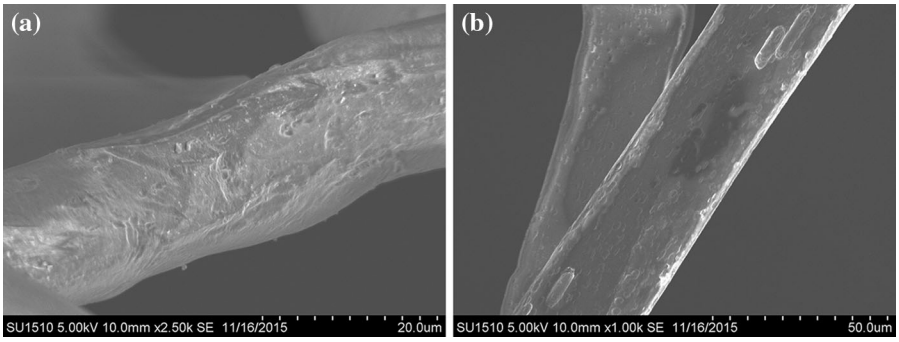

Fig. 5 **a** STF after 90 days in alkaline solution. **b** PET fibers after 90 days in alkaline solution

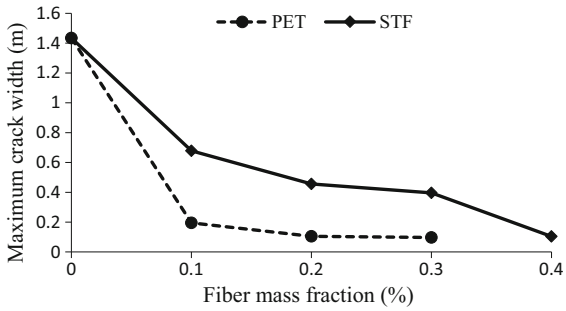

Fig. 6 Maximum crack width

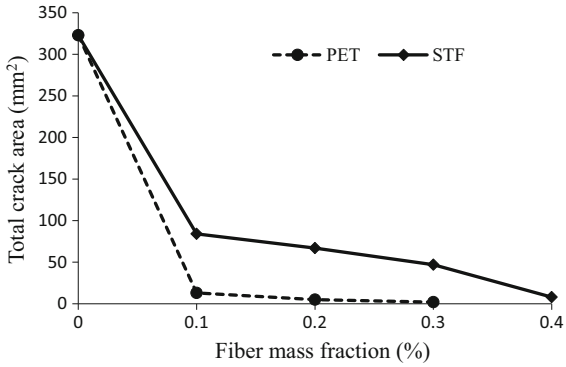

Fig. 7 Total crack area in specimens

capillary pressure is another factor which could have contributed to the decreased cracking observed. Wang et al. [21] reported that macro pores at fiber-matrix interfaces could cause a reduction in matrix capillary pressure thereby decreasing plastic shrinkage cracking.

Given the findings by Raghavan et al. [22] which suggested that scrap tire rubber particles enhance plastic shrinkage resistance of cement mortar, it was expected that the performance of mixtures reinforced with crumb rubber-bearing STF would be better than those of PET reinforced specimens. However, contrary result was observed, and the slightly reduced effectiveness of the STF compared to PET fibers in reducing plastic shrinkage cracking is attributed to the following factors counteracting whatever inherent benefit from crumb rubber. First, the presence of attached crumb rubber particles in the STF fluffs caused fibers to entangle, hence the dispersion of STF during mixture preparation was difficult and the distribution in the matrix could have been inhomogeneous. Moreover, given that fiber addition to mortar was by mass, crumb rubber attachment to STF, made the actual fiber content of mixtures to be lower than those of PET fiber reinforced mortar mixtures. Moreover, the shorter length of STF is another factor which affected its performance. Consequently, in STF reinforced mixtures, reduced length/number of fibers and the associated increased fiber spacing made crack abridgement in specimens slightly less effective in comparison to specimens containing PET fibers.

3.4 Microstructure

Results shown in Fig. 8 indicates that while the ultrasonic pulse velocity through the reference and the STF reinforced specimens were similar at all test ages, they were both lower than those of the specimens containing PET fibers. It is also shown in Fig. 8 that at the end of the first 28 days of accelerated hot-water curing, the ultrasonic pulse velocity across all the samples dropped by approximately 1.5%. It is suspected that changes in pore structure and microcracking due to thermal expansion of pore water and the associated volume change as the temperature of already hardened specimens suddenly increased from 23 to 60 °C is partly responsible for the slightly reduced UPV values observed. According to Reinhardt and Stegmaier [23], increasing steam-curing temperature transforms pore size distribution in concrete to coarser pores, and this is more pronounced in high w/c ratio mixtures. Hence, pore enlargement would invariably cause the transmission time of ultrasonic pulse waves across specimens to increase thereby reducing UPV values.

However, the reversal in UPV trend observed after the first 28 days of hot-water curing is traceable to the constancy of temperature overtime which precludes further pore coarsening. Moreover, increased hydration engendered by the hot-water curing of samples

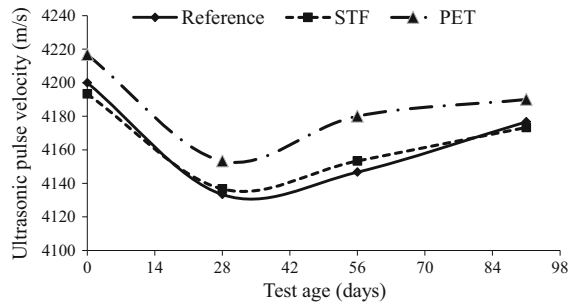

Fig. 8 Effect of accelerated curing on ultrasonic pulse velocity

equally contributed in densifying the matrix thereby gradually improving the microstructure of all specimens with test age. The 91 days UPV values of all the specimens were approximately 99.5% of the moist-cured 28 days values. Given the similar UPV trend observed in the three mixtures investigated, it seems that contaminants attached to STF may not have had any deleterious effect on mortar microstructure. Further discussion on the microstructural changes in specimens is presented in Sect. 3.5

3.5 Phase evolution

Volume changes due to delayed calcium aluminate trisulfate hydrate (ettringite) formation in hardened cement composites have been shown to cause expansion and micro-cracking [24, 25]. However, the rate of ettringite formation is greatly influenced by the availability of sulfate and alumina sources in a cement matrix and the interaction of these aforementioned with cement phases. The results of the SEM–EDS analyses obtained at the end of 90 days exposure of samples to 60 °C hot-water curing are shown in Figs. 9, 10, 11 and 12, and it consist of atomic (molar) ratio plots of the principal elements of hydration phases with respect to calcium. Pure concentrations of ettringite and monosulfate (AFt and AFm hydrate phases, respectively) were not detected in Figs. 9 and 10, rather calcium silicate hydrate (CSH) was the main phase identified. The data cluster of the calcium silicate hydrate (CSH) phase in both mixtures is interspersed with significant traces of portlandite (CH) and minor traces of AFt and AFm phase overlaps. While Si/Ca data cluster for the reference mixture

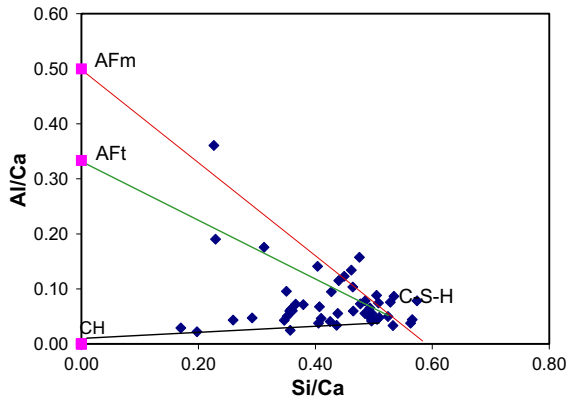

Fig. 9 Reference EDS plot of Al/Ca against Si/Ca

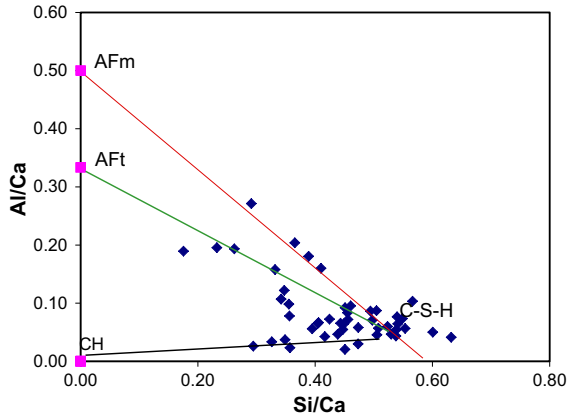

Fig. 10 STF EDS plot of Al/Ca against Si/Ca

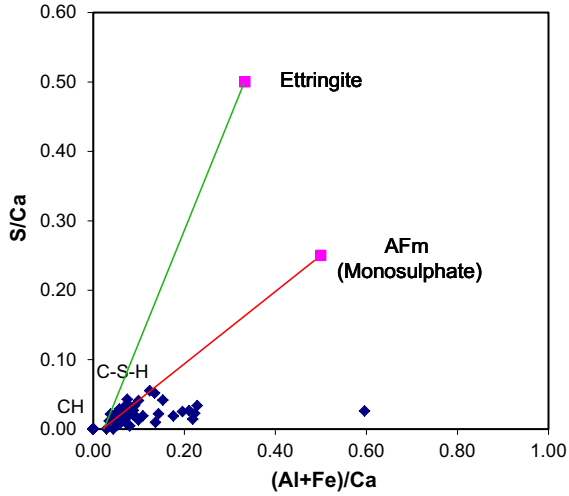

Fig. 11 Reference EDS plot of S/Ca against (Al + Fe)/Ca

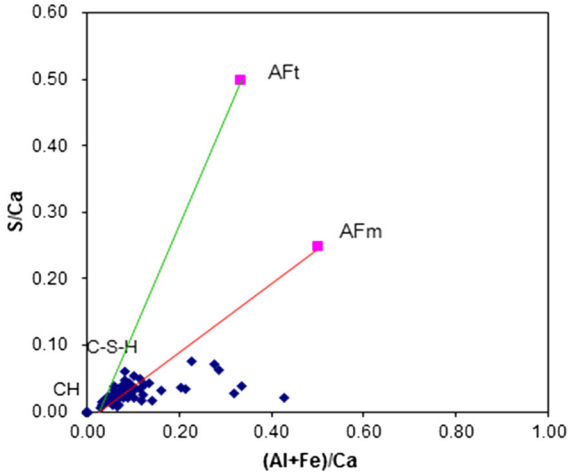

Fig. 12 STF EDS plot of S/Ca against (Al + Fe)/Ca

ranged from 0.35 to 0.0.57, that of the STF mixture was 0.39–0.54. Moreover, excluding a few outliers, the Al/Ca ratios for both mixtures is also similar, and approximately 0.02–0.2.

The absence of pure AFt and AFm phases in these specimens was also made clearer by the information provided in Figs. 11 and 12. However, it seems that there is a slight increase in AFm phase intermixture (higher S/Ca and (Al + Fe)/Ca ratios) in the STF samples shown in Fig. 12 compared to that of the reference mixture shown in Fig. 11. While the S/Ca ratio of the CSH data cluster of the STF samples is approximately 0.08, the value for the reference mixture is about 0.06. On the other hand, the (Al + Fe)/Ca ratio of the STF samples is 0.33 compared to the 0.23 obtained for the reference samples. The slightly increased S/Ca and (Al + Fe)/Ca ratios of the STF samples is traceable to contaminants attached to STF. Whereas the unremoved steel fibers attached to STF contributed to the increase in (Al + Fe)/Ca ratio, the slight increase in S/Ca ratio is attributed to the presence of sulfur-bearing crumb rubber particles. The XPS narrow scan spectrum shown in Fig. 4 confirmed that sulfur is present in crumb rubber as thiophenic and sulfate.

While the slightly increased intermixing of monosulfate in the STF specimens is of concern, its potentially debilitating effect is counteracted by the infinitesimal amount of internal sulfates in the STF specimens. Hence, high volume formation of expansive ettringite in specimens appears improbable. Apparently, this is why sulfate enrichment of CSH or decalcification of calcium from the CSH which would have been highlighted by substantially increased S/Ca ratio in the STF reinforced samples was not observed in this study.

3.6 Mechanical strength development

The strength evolution of samples exposed to 60 °C hot-water curing is shown in Fig. 13. Increases in the strength of specimens with age were observed in all the samples. With the exception of the first 28 days of immersion in hot-water, the UPV and compressive strength results appears to be in agreement, confirming the absence of volume expansion and matrix microcracking usually induced by the moisture adsorption of ettringite in hardened cement composites.

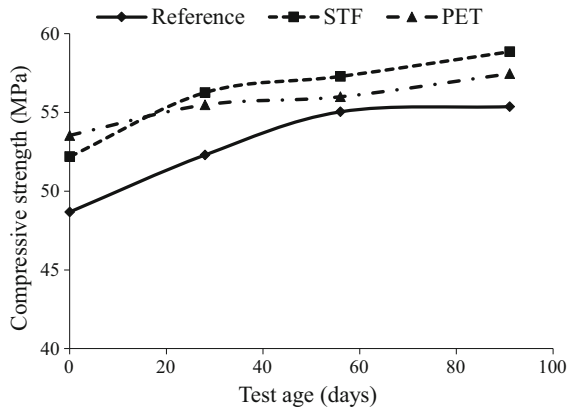

Fig. 13 Effect of accelerated curing on strength evolution

Moreover, Fig. 13 also showed that the strength gain of the fiber reinforced specimens was lower than those of the reference specimen at 90 days. The percentage increase in strength of specimens relative to the 28th day moist cured strength are 13.7% for the reference, 12.8% for the STF specimens and 7.3% for the PET fiber reinforced specimens. This development is surprising given that PET fiber reinforced specimens which had no sulfate-bearing crumb rubber inclusions, and with the highest compressive strength at 28 days of moist curing recorded the lowest strength gain. It seems that while increased hydration due to sustained 60 °C hot-water curing overtime caused an unimpeded strength enhancement of the reference specimens, it also improved the strength of the fiber reinforced specimens albeit with a slight modification of the fibers and the fiber-matrix interface. Hence, as a consequence of changes in fiber/fiber-matrix interface, the crack bridging capacity of these fibers became enfeebled. Li et al. [26] investigated the performance of polyvinyl alcohol (PVA) reinforced cement composites after a 26 weeks immersion in a 60 °C hot water, and they reported reductions in apparent fiber strength, modulus of elasticity, strain capacity and fiber bridging property. Compared to the PET fibers, the mechanical performance of STF reinforced specimens suggest that hot water curing had minimal effect on STF fibers, and this could be probably as a result of surface coating deposited on these fibers during the tire manufacturing process. Compared to PET fibers, the higher stability of STF under hot-water curing condition appears to be similar to its performance in alkaline solution reported in Sect. 3.2. All in all, these test results indicate that the attachment of sulfur-

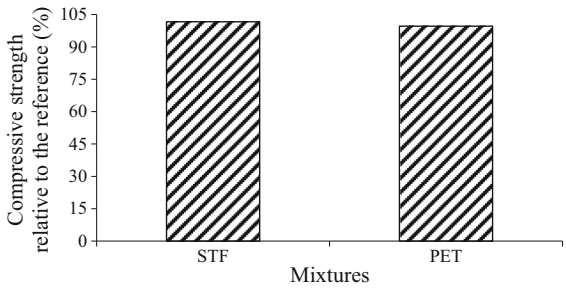

Fig. 14 Percentage compressive strength relative to that of reference after sulfate exposure

bearing crumb rubber particles to STF did not undermine the long-term strength of cement composites.

3.7 Longitudinal expansion and sulfate resistance

After 3 months of exposure to 60 °C hot-water curing environment, no longitudinal expansion of specimens was observed. Furthermore, compared to the plain reference and PET reinforced mortar specimens immersed in Na_2SO_4 solution for 3 months, Fig. 14 shows that the addition of STF to mixtures did not reduce the compressive strength of mortar specimens immersed in the same acidic solution. These two test results are in agreement with the results reported in the previous sections, thus confirming the benign nature of the crumb rubber particles contained in the STF utilized in this study. However, it is emphasized that these findings are related to only 0.4% STF addition level, the sulfate induced degradation implication of incorporating significantly higher quantities of STF/crumb rubber particles to mortar is unknown at present.

4 Conclusions

In this study, STF was physically and chemically characterized, and its stability in alkaline environment evaluated. The effects of STF on plastic shrinkage cracking, microstructure and long-term durability of mortar mixtures were also investigated. Based on the experimental results obtained in this study, the following conclusions are drawn:

- STF consist mainly of polyester fibers measuring approximately 3–5 mm in length and 18–20 μm in width. Moreover, surface layer of some of the STF are scarified, and the crumb rubber inclusions found attached to STF are also sulfate-bearing.
- Both STF and PET fibers degrades in alkaline environment; however deterioration was less severe for the STF fibers as a result of the presence of adhesive coating on its surface.
- The plastic shrinkage crack resistance of cement mortar was enhanced by the addition of 0.4% STF. The reduction in total crack area relative to the plain unreinforced mortar was approximately 92.7%. A performance comparable to that of mortar reinforced with 0.3% commercial PET fibers.
- At 0.4% STF addition level, the sulfate-bearing crumb rubber particles attached to STF was too insignificant to cause sulfate induced deleterious effect on mortar microstructure. Furthermore, longitudinal expansion test, ultrasound and sulfate resistance test indicate that STF addition to mixtures did not impair the durability of mortar specimens.
- While further studies are required to evaluate the performance of other types of polymeric scrap tire fibers, as well as the effects of higher STF content in mixtures and hybrid combinations of STF and other synthetic fibers, the present study indicates a huge potential for PET-based STF as a microfiber reinforcement for repair mortar applications.

Acknowledgements The authors are grateful for the financial support extended by the Tire Stewardship British Columbia (TSBC) and Western Rubber Products, Ltd. Discussions with Mr. Nick Winter with respect to EDS analyses is also greatly appreciated.

Compliance with ethical standards

Conflict of interest While Obinna Onuaguluchi has no conflicts of interest. Nemkumar Banthia has received research Grants from Tire Stewardship British Columbia (TSBC) and Western Rubber Products, Ltd.

References

1. Tire Stewardship British Columbia (TSBC) (2015) Annual report to the director, Waste Prevention. Retrieved on 22nd January 2017: from: https://www.tsbc.ca/pdf/TSBC-AnnualReport2015.pdf
2. Chen JH, Chen KS, Tong LY (2001) On the pyrolysis kinetics of scrap automotive tires. J Hazard Mater B84:43–55

3. Levendis YA, Atal A, Carlson J, Dunayevskiy Y, Vouros P (1996) Comparative study on the combustion and emissions of waste tire crumb and pulverized coal. Environ Sci Technol 30:2742–2754
4. Murena F (2000) Kinetics of sulphur compounds in waste tyres pyrolysis. J Anal Appl Pyrol 56:195–205
5. Tang L, Huang H (2004) An investigation of sulfur distribution during thermal plasma pyrolysis of used tires. J Anal Appl Pyrol 72:35–40
6. Banthia N, Gupta R (2006) Influence of polypropylene fiber geometry on plastic shrinkage cracking in concrete. Cem Concr Res 36(7):1263–1267
7. Naaman AE, Wongtanakitcharoen T, Hauser G (2005) Influence of different fibers on plastic shrinkage cracking of concrete. ACI Mater J 102(1):49–58
8. Najm H, Balaguru P (2002) Effect of large-diameter polymeric fibers on shrinkage cracking of cement composites. ACI Mater J 90(4):345–351
9. Thomas BS, Gupta RC (2015) Long term behavior of cement concrete containing discarded tire rubber. J Clean Prod 102:78–87
10. Topçu IB, Demir A (2007) Durability of rubberized mortar and concrete. J Mater Civ Eng 19(2):173–178
11. Ochi T, Okubo S, Fukui K (2007) Development of recycled PET fibre and its application as concrete-reinforcing fibre. Cem Concr Compos 29:448–455
12. Won J-P, Jang C, Lee S-W, Lee S-J, Kim H-Y (2010) Long-term performance of recycled PET fibre-reinforced cement composites. Constr Build Mater 24:660–665
13. ASTM (American Society for Testing and Materials) E1252 (2013) Standard practice for general techniques for obtaining infrared spectra for qualitative analysis. ASTM International, West Conshohocken
14. Banthia N, Gupta R (2007) Test method for evaluation of plastic shrinkage cracking in fiber reinforced cementitious materials. Exp Tech 31(6):44–48
15. ASTM C39 (2015) Standard test method for compressive strength of cylindrical concrete specimens. ASTM International, West Conshohocken
16. Hu H, Fang Y, Liu H, Yu R, Luo G, Liu W, Li A, Yao H (2014) The fate of sulfur during rapid pyrolysis of scrap tires. Chemosphere 97:102–107
17. Huang W, Dong J, Li F, Chen B (2002) Study of the tribological behavior of *S*-(carboxylpropyl)-*N*-dialkyldithiocarbamic acid as additive in water-based fluid. Wear 252:306–310
18. Wang Y, Backer S, Li VC (1987) An experimental study of synthetic fibre reinforced cementitious composites. J Mater Sci 22:4281–4291
19. Silva DA, Betioli AM, Gleize PJP, Roman HR, Gomez LA, Ribeiro JLD (2005) Degradation of recycled PET fibers in Portland cement-based materials. Cem Concr Res 35:1741–1746
20. Jamshidi M, Afshar F, Mohammadi N, Pourmahdian S (2005) Study on cord/rubber interface at elevated temperatures by H-pull test method. Appl Surf Sci 249:208–215
21. Wang K, Shah SP, Phuaksuk P (2001) Plastic shrinkage cracking in concrete materials—influence of fly ash and fibers. ACI Mater J 98(6):458–464
22. Raghavan D, Huynh H, Ferraris CF (1998) Workability, mechanical properties, and chemical stability of a recycled tire rubber-filled cementitious composite. J Mater Sci 33:1745–1752
23. Reinhardt HW, Steigmaier M (2006) Influence of heat curing on the pore structure and compressive strength of self-compacting concrete (SCC). Cem Concr Res 36:879–885
24. Collepardi M (2003) A state-of-the-art review on delayed ettringite attack on concrete. Cem Concr Compos 25:401–407
25. Lawrence CD (1995) Mortar expansions due to delayed ettringite formation. Effects of curing period and temperature. Cem Concr Res 25(4):903–914
26. Li VC, Horikoshi T, Ogawa A, Torigoe S, Saito T (2004) Micromechanics-based durability study of polyvinyl alcohol engineered cementitious composites. ACI Mater J 101(3):242–248